Science of the Total Environment 409 (2011) 3059–3065

Contents lists available at ScienceDirect

Science of the Total Environment

journal homepage: www.elsevier.com/locate/scitotenv

The influence of biofilms on the migration of uranium in acid mine drainage (AMD) waters

E. Krawczyk-Bärsch [a,*], H. Lünsdorf [b], T. Arnold [a], V. Brendler [a], E. Eisbein [c], U. Jenk [d], U. Zimmermann [d]

[a] Helmholtz-Zentrum Dresden-Rossendorf, Institute of Radiochemistry, P.O. Box 51 01 19, D-01314 Dresden, Germany
[b] Helmholtz Centre for Infection Research, Department of Vaccinology and Applied Microbiology, Inhoffenstr. 7, D-38124 Braunschweig, Germany
[c] TU Bergakademie Freiberg, Institute of Physical Chemistry, Akademiestraße 6, D-09596 Freiberg, Germany
[d] Wismut GmbH, Jagdschaenkenstr. 29, D-09117 Chemnitz, Germany

ARTICLE INFO

Article history:
Received 3 February 2011
Received in revised form 30 March 2011
Accepted 27 April 2011

Keywords:
AMD water
Uranium
Biofilm
Ferrovum myxofaciens
Microsensor measurement

ABSTRACT

The uranium mine in Königstein (Germany) is currently in the process of being flooded. Huge mass of *Ferrovum myxofaciens* dominated biofilms are growing in the acid mine drainage (AMD) water as macroscopic streamers and as stalactite-like snottites hanging from the ceiling of the galleries. Microsensor measurements were performed in the AMD water as well as in the biofilms from the drainage channel on-site and in the laboratory. The analytical data of the AMD water was used for the thermodynamic calculation of the predominance fields of the aquatic uranium sulfate (UO_2SO_4) and UO_2^{++} speciation as well as of the solid uranium species Uranophane [$Ca(UO_2)_2(SiO_3OH)_2{\cdot}5H_2O$] and Coffinite [$U(SiO_4)_{1-x}(OH)_{4x}$], which are defined in the stability field of pH>4.8 and Eh<960 mV and pH>0 and Eh<300 mV, respectively. The plotting of the measured redox potential and pH of the AMD water and the biofilm into the calculated pH–Eh diagram showed that an aqueous uranium(VI) sulfate complex exists under the ambient conditions. According to thermodynamic calculations a retention of uranium from the AMD water by forming solid uranium(VI) or uranium(IV) species will be inhibited until the pH will increase to >4.8. Even analysis by Energy-filtered Transmission Electron Microscopy (EF-TEM) and electron energy loss spectroscopy (EELS) within the biofilms did not provide any microscopic or spectroscopic evidence for the presence of uranium immobilization. In laboratory experiments the first phase of the flooding process was simulated by increasing the pH of the AMD water. The results of the experiments indicated that the *F. myxofaciens* dominated biofilms may have a substantial impact on the migration of uranium. The AMD water remained acid although it was permanently neutralized with the consequence that the retention of uranium from the aqueous solution by the formation of solid uranium species will be inhibited.

1. Introduction

In the uranium mine of the Wismut GmbH near Königstein (Saxony, Germany) the uranium production was achieved by leaching the sandstone with sulfuric acid. As a consequence the geochemical nature of the drainage water of the deposit was changed leading to an increase in sulfate and heavy metal concentration. For remediation purposes the mine is currently in the process of being flooded since 2001. The flooding water is collected and pumped out of the mine. It is treated on the surface by a conventional water treatment plant. In small drainage channels thick biofilms have formed and occur as gelatinous filaments (Fig. 1a), described in the literature as “macroscopic streamers” (Hallberg et al., 2006). Stalactite-like biofilms with a maximum length of 45 cm were hanging from the ceiling of the galleries (Fig. 1b). They consisted of a solid mineral basis whereas the most part appeared to be mucilaginous. Mine water was dripping from the ceiling and percolating the biofilms. Pisarowicz and de Villa Luz (1994) was the first who called the stalactitic form “snottite” on the basis of their appearance and texture in the Cueva de Villa Luz (southern Mexico). Acidophilic Fe (II)-oxidizing bacteria were contributing there as primary producers to the bacterial community. In a recent work Ziegler et al. (2009) described snottites as a novel bacterial pyrite leaching community from the ‘Drei Kronen und Ehrt’ field site in the Harz Mountains (Germany). The bacterial diversity of the streamers and the snottites of the abandoned underground uranium mine in Königstein is similar. As described by Brockmann et al. (2010) the identification on the basis of 16S rDNA sequences showed a dominance of *Ferrovum myxofaciens*, an acidophilic, autotrophic, iron oxidizing bacteria, which belongs to the *Betaproteobacteria*. Even in water samples from an open drainage channel of the uranium mine, analyzed by fluorescence in situ hybridization (FISH) and terminal restriction fragment length polymorphism (T-RFLP), a dominance of these bacteria was found (Seifert et al., 2008).

Since the microbial community thrives in high amounts in the AMD water of the uranium mine the question is posed how they may influence

* Corresponding author. Tel.: +49 351 2602076; fax: +49 351 2603553.
E-mail address: E.Krawczyk-Baersch@hzdr.de (E. Krawczyk-Bärsch).

0048-9697/$ – see front matter © 2011 Elsevier B.V. All rights reserved.
doi:10.1016/j.scitotenv.2011.04.051

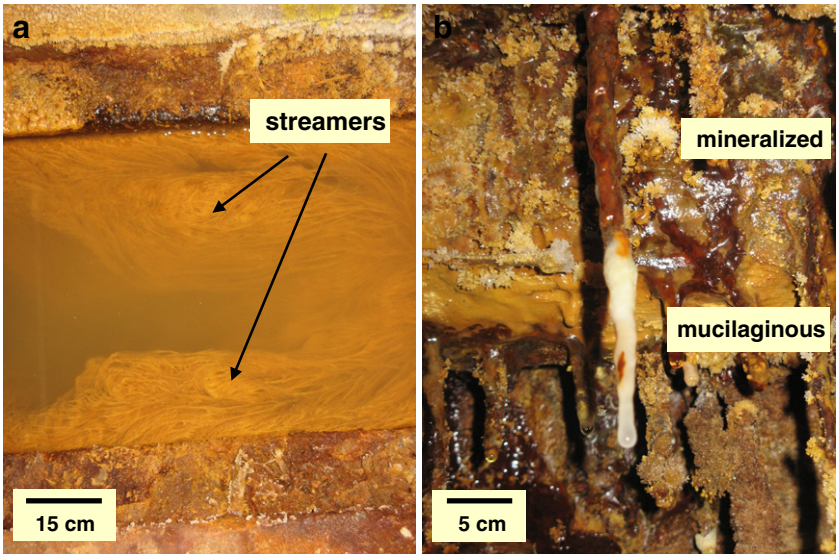

Fig. 1. Gelatinous filaments, so-called macroscopic streamers (a) in the AMD water, and stalactite-like snottites (b), hanging from the ceiling of the galleries.

the immobilization of uranium in respect to their bioremediation potential. It is known that biofilms can provide a sink for dissolved heavy metals (Späth et al., 1998) due to the fact that the exopolymeric substances (EPS), cell walls, cell membranes and cell cytoplasm can serve as sorption sites (Flemming, 1995). Several mechanisms of interactions of microorganisms with radionuclides under aerobic conditions are known as biosorption (e.g. Pons and Fusté, 1993), interactions with S-layers (e.g. Merroun et al., 2005), bioprecipitation (e.g. Macaskie et al., 2000) or microbial reduction of uranium(VI) (e.g. Abdelouas et al., 1998; Beyenal et al., 2004). Some of these mechanisms have the potential for a substantial retention of uranium. However, little is known about the retention processes of heavy metals in a microbial community, such as biofilms. In a recent work by Grossmann et al. (2007) uranium(V) and uranium(VI) precipitates have been identified as microparticles in a pH neutral multispecies biofilm indicating the reduction of uranium. However, for the interpretation of retention processes in biofilms the determination of the in-situ microbial metabolic processes is useful since these metabolic processes are sensitive to metals and their speciation. Changes of redox potential, pH and oxygen will have an effect on the bioavailability of the metals in a complex manner. To characterize these geochemical parameters for further interpretation, biofilms of the uranium mine "Königstein" were studied on-site for the first time and after sampling in the laboratory by redox potential and pH microsensors. The used microsensors are characterized by a sensor tip diameter of a few micrometers, which allows pH and redox potential measurements of a fine scale. With such measuring device chemical gradients have been described in recent studies, performed in heterogeneous or homogeneous natural environments (e.g. de Beer, 2000; Kühl, 2005; Krawczyk-Bärsch et al., 2008; Revsbech, 2005). The results of the sensor measurements in the uranium mine "Königstein" should provide an answer to the question if uranium is immobilized in the biofilms as well as in the surrounding water of the uranium mine under the ambient conditions and in the first phase of the flooding process. Supporting methods are microscopy and spectroscopy as well as thermodynamic calculations of analytical data for the construction of a system for stability fields of uranium species.

2. Experimental

2.1. Sampling

Biofilm and water samples were taken from a gallery of pit 390 at +50 m above sea level of the uranium mine, which was accessible for inspections and sampling campaigns. Biofilms from the drainage channel, the so-called macroscopic streamers, were sampled in March 2010 in sterile 250 ml boxes, whereas the AMD water samples were collected in sterile 1 l glass bottles for anion and cation analysis. For EF-TEM/EELS studies snottites were removed from the ceiling. They were fixed in-situ with 1% (vol/vol) glutardialdehyde by mixing 0.6 ml glutardialdehyde (25% vol/vol) with 14.4 ml AMD water, which was dropping down the snottites. The fixed snottites were transported in a small (15 ml) tube for further preparation in the TEM laboratory. The dropping water was collected for analysis, too.

2.2. Water analysis

The AMD water from the drainage channel and the water, which was dropping down the snottite-biofilm were sampled for analysis. After the determination of the pH it was acidified and analyzed for determination of the inorganic elements by Inductively Coupled Plasma Spectrometry (ICP-MS) using an ELAN 9000 type ICP-MS spectrometer (Perkin Elmer, Überlingen, Germany) and an AXIOM type ICP-MS spectrometer (VG Thermo Elemental, Winsford, UK). The anions were determined by Ion Chromatography using the IC-system 732/733 (Metrohm, Filderstadt, Germany). Total organic carbon (TOC) was determined with the *HT1300-TOC* equipment (Analytik Jena, Jena, Germany).

2.3. Microsensor measurements

Microsensor measurements were performed in the biofilms from the drainage channel on-site and in the laboratory by using redox potential and pH electrodes. For redox potential measurements a miniaturized platinum electrode (Unisense, Aarhus, Denmark) with a tip diameter of 10 µm was connected via a high-impedance millivoltmeter to a reference electrode, a simple open-ended Ag/AgCl electrode with a gelstabilized electrolyte. The redox microelectrode was checked for its function by different quinhydrone redox buffer as described in Vilalta and Sabater (2005). After the measurements the obtained values were corrected using a correction factor after Stumm and Morgan (1996), which is dependent on the temperature and the molar concentration of the electrolyte of the reference electrode. Sensor measurements of the pH were performed by a miniaturized conventional pH electrode from Unisense with a tip

diameter of 10 μm. The pH electrode was connected via a high-impedance millivoltmeter to a separate reference electrode as described before and calibrated by using commercially available buffers. The redox potential and pH sensors were fixed in a holder on a motor-driven micromanipulator stage, connected with a motor controller for a precise small-scale positioning and for automated measurements in 50 μm steps within the biofilms. A number of microprofilings were performed in the biofilm, starting the measurements at the biofilm/water–air interface and becoming progressively immersed into deeper zones of the biofilm towards the center.

For sensor measurements in the laboratory the biofilm samples were positioned in a self-constructed rectangular flow cell with an outer dimension of 121×42×15 mm. During the measurements the AMD water was pumped through the flow cell in a closed circuit with a flow velocity of 4 ml/min, simulating the condition on-site. In these experiments the first phase of flooding of the mine was simulated by increasing the pH of the AMD water to a neutral pH by adding 1 M NaOH, while the water was pumped through the biofilm in a closed circle under non-sterile conditions. The pH of the water was measured twice the day during 95 h and was readjusted to 6.45–6.80 since it decreased permanently <4. Redox potential and pH measurements were performed in the biofilm and in the water after 20 and 95 h, respectively. The experiments were limited by the duration of 95 to exclude changes in the microbial diversity of the sampled biofilms due to the influence of environmental bacteria, which exist in the laboratory. This process was described by Krawczyk-Bärsch et al. (2008) when conducting experiments under non-sterile conditions in the laboratory.

2.4. Energy-filtered Transmission Electron Microscopy (EF-TEM)

Different portions of the snottite, e.g. surface-near, central and intermediate, were excised and processed further, following the routine embedding protocol with minor modifications as described by Lünsdorf et al. (2001). Samples were washed twice in 20 mM Hepes, pH 7.2 for 5 min. Samples were dehydrated in an ascending ethanol series (10, 30, 50, 70, 90, 100% for 20 min on ice; 100% for 15 min at ambient temperature) followed by resin impregnation and polymerization in ERL-resin (Spurr, 1969). 35 to 40 nm ultrathin sections were electron spectroscopically analyzed with an in-column filter EF-TEM (LIBRA 120plus, Zeiss, Oberkochen, Germany) at magnifications from ×4000 to ×50,000, with an energy-setting as described in Lünsdorf et al. (2001).

2.5. Microscopical investigations of stained biofilm

For live-dead staining the biofilm (65 mg dry biomass) was treated for 2 min in the dark with 20 μl of the red-fluorescent nucleic acid stain, propidium iodide from Molecular Probes, Inc. (Eugene, USA). The stock solution (1 mg/ml) was diluted before with the factor 1:10 in PBS. The biofilm samples were counterstained with 300 μl of a dye solution of the DNA-binding fluorochrome 4,6-diamidino-2-phenylindole (DAPI) for 60 min. The dye solution was prepared before from a stock solution of DAPI (1.0 mg/ml) purchased from Molecular Probes. For microscopical examinations a LEICA Confocal Laser Scanning Microscope (TCS-SP2) was used, equipped with a mercury lamp. Detailed views were performed with lenses from LEICA (HCX PL APO 63×/1.20 W CORR). When excited with UV at 351 or 364 nm, DAPI fluoresces in the blue to cyan range at 461 nm. Whereas DAPI will pass through an intact cell membrane propidium iodide penetrates only bacteria with damaged membranes (Wilson et al., 1990). The fluorescence excitation maximum for propidium iodide is 535 nm. It was excited with the 488 nm line of an argon–ion laser.

3. Results and discussion

3.1. Thermodynamic calculation

Analysis from the dripping water of the snottites and the drainage channel water showed high uranium concentrations of 59.51 mg/L (2.50×10^{-4} M) and 10.4 mg/L (4.37×10^{-5} M), respectively (Table 1). The analytical data of the drainage water was used for the calculation of the predominance fields of different uranium species in the pH–Eh diagram for the U–S–O–H–C system at 15 °C by using the geochemical speciation code "Geochemist's Workbench" Version 8.0.8/ACT2 Version 8.0.8. By means of the equilibrium speciation model the speciation of the uranium metal can be determined, and changes in the concentration of the various species with changing conditions of redox potential, pH, temperature, ionic strength, and solid mineral phases can be related to changes in the behavior of the microbes. The default data base used was the thermo.dat accompanying the code, supplemented by the most recent NEA database for uranium (Guillaumont et al., 2003), and by solubility data for Uranophane (Nguyen et al., 1992), Soddyite (Gorman-Lewis et al., 2007), Na-Compreignacite (Gorman-Lewis et al., 2008), Boltwoodite (Clark et al., 1998), Na-Boltwoodite (Nguyen et al., 1992), Meta-Schoepite (Guillaumont et al., 2003), and Haiweeite (Chen et al. (1999). The theoretical predominance fields of solid uranium species under the ambient condition found in the AMD are clearly defined in two geochemically different areas: The first area is characterized by a redox potential of approximately <300 mV and a pH, which varies between 0 and 7.4. Assuming reducing conditions, the formation of the uranium(IV) mineral Coffinite $[U(SiO_4)_{1-x}(OH)_{4x}]$ was predicted. The second area is characterized by a pH>4.8 and a redox potential ≤960 mV and is dominated by the calcium bearing uranium-hydro-silicate Uranophane $[Ca(UO_2)_2(SiO_3OH)_2{\cdot}5H_2O]$. Since Haiweeite was included in the thermodynamic calculation the predicted stability field for this phase replaced most of the field for Uranophane. However, as described in Chen et al. (1999) Uranophane is more stable than Haiweeite under most geochemical conditions and therefore frequently found in nature. Due to this fact it seemed more informative to use the stability field of Uranophane for our studies.

3.2. Microsensor measurements

In our studies the formation of solid uranium phases in the biofilms and in the AMD water was theoretically proved by plotting redox potential and pH values into the thermodynamically calculated pH–Eh diagram for the U–S–O–H–C system. Sensor measurements of the redox potential and pH were performed for this purpose on-site within the macroscopic streamers and in the snottites as well as in the drainage water and in the water dripping from the snottites. Microprofilings started at the biofilm/water–air interface of the snottite, which was fixed in a self-constructed holder. The first measuring point was depicting a redox potential of the water of 728 mV ± 10 mV, which was confirmed by separated measurements in the collected AMD water. Measurements in the dripping water from the snottites showed similar values of a redox potential of 718 mV ± 8 mV. As soon as the electrode penetrates into the snottite the redox potential got stabilized showing a value of 802 ± 9 mV. Finally, in the center of the snottite a high redox potential of 834 ± 10 mV was detected. Redox potential measurements performed in the macroscopic streamers of the drainage channel showed higher values in the center of the biofilm of 921 ± 17 mV. High redox potentials in biofilms, which are dominated by acidophilic Fe(II)-oxidizing bacteria, are in general not unusual. Fe(II)-oxidizing bacteria are known for its ability to use ferrous iron compounds at potentials of up to + 700 mV and above (Rawlings et al., 1999). The pH of the macroscopic streamer and the snottite was very low (1.9–2.2). In comparison, the pH of the dripping water of the snottites and the pH

Table 1
Mean concentration of cations and anions in the AMD channel water and in the water dripping from the snottites. Sample campaign March 2010.

	AMD channel water [in mg/l]		Dripping water of snottites [in mg/l]	
Na	22.3	20.1–23.1	36.1	31.9–37.7
Mg	11.8	11.4–12.3	19.5	19.0–20.4
Al	16.8	16.6–17.2	61.1	60.2–61.4
Si	15.6	15.2–16.1	24.5	24.2–25.3
P	<0.01	<0.01	<0.01	<0.01
K	13.9	11.9–14.5	10.4	10.1–10.6
Ca	122	119–126	170	167–176
Cr	<0.05	<0.05	0.2	0.19–0.21
Mn	3.73	3.69–3.8	9.55	9.4–9.9
Fe	20.7	20.2–21.5	290	284–296
Co	0.14	0.14	0.642	0.635–0.647
Ni	0.31	0.30–0.31	1.06	1.04–1.10
Cu	<0.01	<0.01	0.092	0.09–0.094
Zn	6.45	6.43–6.51	17.78	17.4–18.0
As	<0.01	<0.01	0.0365	0.0358–0.0368
Sr	0.747	0.742–0.76	1.15	1.14–1.16
Cd	0.0563	0.0552–0.06	0.358	0.356–0.36
Cs	<0.006	<0.006	<0.01	<0.01
Ba	<0.01	<0.01	<0.001	<0.001
Pb	0.273	0.269–0.275	0.185	0.17–0.191
U	10.5	10.4–10.6	59.51	59.1–60.6
Chloride	26.9	26.6–27.8	43.1	42.5–43.3
Nitrate	<2	<2	<2	<2
Phosphate	<5	<5	<5	<5
Sulfate	767	761–771	2053	2020–2100

of the AMD water of the channel were characterized by a higher pH of 2.56 ± 0.1 and 2.86 ± 0.1, respectively.

The results clearly showed significant differences between the geochemical parameters of the biofilms and the waters, indicating that biofilms have built up their own microenvironments. In these microenvironments the bioremediation potential of biofilms will change with redox potential, pH, and oxygen. For estimating the bioremediation potential of the studied biofilms, the results of the redox potential were plotted together with the pH into the calculated pH–Eh diagram for the U–S–O–H–C system. As shown in Fig. 2, the plots appear in the area of aqueous solution, indicating that an aqueous uranium(VI) sulfate complex exists under these conditions in the biofilms according to the thermodynamic calculations. The same result was achieved by plotting the redox potential and pH values of the AMD water and the dripping water of the snottite into the diagram. In fact, a highly mobile aquatic uranium sulfate species $UO_2SO_{4(aq)}$ was determined in the AMD water by previous time-resolved laser-induced fluorescence spectroscopy studies (TRLFS) by Arnold et al. (2011).

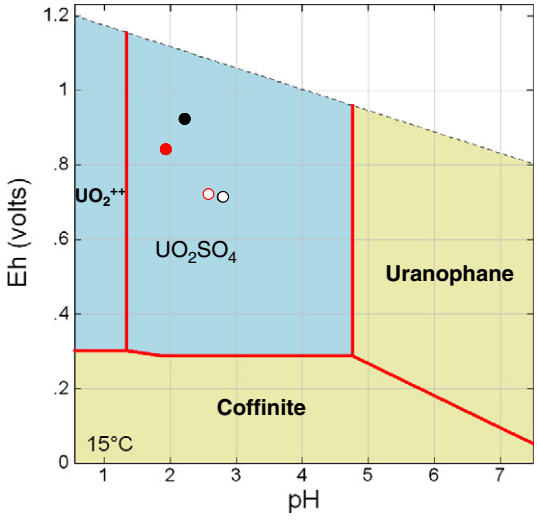

Fig. 2. ph–Eh diagram for U–S–O–H–C system at 15 °C. Eh and pH values, measured within the macroscopic streamers (●) and within the snottite (●), were plotted into the diagram as well as data of the AMD water of the channel (○) and the dripping water from the snottites (○). Each of the plots is located in the field of aqueous uranium(VI) sulfate complexation.

3.3. Energy-filtered Transmission Electron Microscopy (EF-TEM)

However, due to the complexity of biological systems the possibility of the retention of uranium, e.g. by polymers of the extra cellular matrix of the biofilm, should not be excluded until further studies have been proved. EF-TEM offers the possibility to systematically study and analyze the ultra structure and elemental composition of nanoscale mater by electron energy loss spectroscopy (EELS). For this purpose snottites were used, being most suitable for the EF-TEM preparation due to their consistency. In different cross sections individual bacterial cells of *F. myxofaciens* with a dimension of approximately 600 nm in length and 400 nm in width were observed as the dominant microorganism. Between the single cells small crystallized precipitates (40 nm in diameter) were observed as clusters in the cell's vicinity. These colloids were not observed in the open water channels, the so-called voids, where nutrients from the AMD water infuse into the biofilm to the microorganisms and their metabolites and exudates are released (Stoodley et al., 1994). Further precipitates were observed to be associated with the bacterial cell surface. Ultra structural and EELS analysis, shown in Fig. 3 revealed characteristic thin-layered electron dense deposits on the bacterial surface (Fig. 3, a–d), mainly composed of iron and oxygen (Fe-L_{3max}: 708.7 eV, Fe-L_{2max}: 722.5 eV; O-K_{max}: 738.5 eV). The occurring process is described in Kirby et al. (1999) as the result of a biologically catalyzed rapid oxidation in acidic waters following the equation:

$$Fe^{2+}_{(aq)} + 0.25O_{2(aq)} + H^{+}_{(aq)} \Leftrightarrow Fe^{3+}_{(aq)} + 0.5H_2O \quad (1)$$

The process is microbiologically driven by the activity of the Fe oxidizing bacteria, which gain their energy from the proton gradient across the cellular membrane and subsequent iron oxidation. They are promoting the oxidation and precipitation of iron in AMD waters resulting in the remediation of acidic mine drainage waters (Hallberg and Johnson, 2003). Meta-stable and poorly crystallized Fe mineral phases, mostly schwertmannite ($Fe_8O_8(SO_4)(OH)_6$) with additional jarosite ($KFe_3(SO_4)_2(OH)_6$) and/or goethite (FeOOH) may form as precipitates dependent on the water pH (2–4) of the acid sulfate rich water (España et al., 2005, Ziegler et al., 2009). In the present case no K^+, NH_4^+ or Na^+ as relevant cations of jarosite could be detected in the snottite by EELS. Similarly sulfur (with its SO_4^{2-} fingerprint) could not be detected, which gives evidence that sulfur is only a minor constituent of the iron–oxy-precipitates although analysis of the water, which was dropping from the ceiling and penetrating the snottites, showed a sulfate concentration of approximately 2400 mg/l (Table 1). We assume that in the determined mucilaginous part of the snottite the formation of jarosite has not yet taken place. In respect to the high concentration of uranium in the dripping water of the snottites and in the AMD water of the drainage channels the capacity of uranium in the snottites was recorded by EELS from adequate electron dense precipitates, associated to the bacterial surface or adjacent to the biofilm/water–air interface. But never uranium ionization intensity peaks of O- and/or N-edges ($O_{4,5} = 93.5$ eV; $N_5 = 714.0$ eV; $N_4 = 754.5$ eV; Reimer et al., 1992) could unequivocally be observed within the instrumental detection limits. As shown in Fig. 3(e) electron-dense matter, deposited on the cell surface, is mainly detected as iron compound. U–N_{45}-characteristic ionization edges were not recognized. However, analysis by TEM/EELS did not

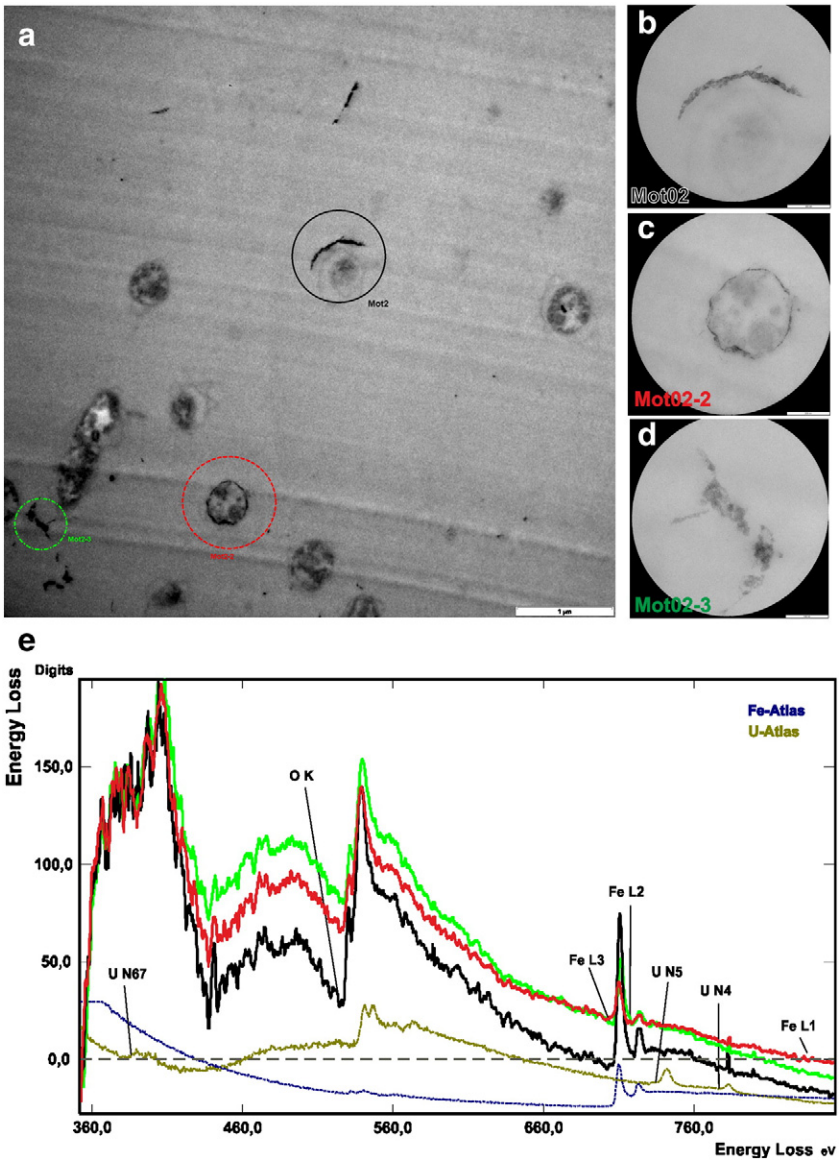

Fig. 3. Ultrastructure of the snottite surface-proximate biomatrix and its elemental characterization by EF-TEM. (a) Cluster of autochthonous bacteria, some of which (circles) have been chosen for EELS analysis. (b, c, d) Ultrastructural detailed views framed by the measuring aperture, which indicate the areas of measurements. (e) Corresponding EELS spectra, colored green, black and red, according to the colored circles in (a). EELS-Atlas reference spectra of Fe and U are shown in blue and dark-yellow.

provide any microscopic or spectroscopic evidence for the presence of uranium immobilization within the investigated biofilms.

3.4. Simulation of the flooding process

Since the uranium mine is currently in the process of being flooded the local geochemical conditions are changing step by step caused by the inflow of water and the closure of the galleries. The pH of the water will probably increase, accompanied by a decrease of the redox potential and oxygen concentration. In laboratory experiments the first phase of flooding was simulated by rinsing samples of macroscopic streamers with neutralized AMD water, which were positioned in a flow cell. The results showed that the neutralization of the AMD water has a significant effect on the redox potential of the biofilm. The primarily measured redox potential of 921 ± 17 mV in the center of the biofilm decreased to 565 ± 5 mV and 433 ± 5 mV after 20 and 95 h, respectively. However, the pH of the biofilm rested acidic, showing 2.8 ± 0.1 and 2.9 ± 0.1 after 20 and 95 h. The results, which were plotted into the calculated pH–Eh diagram for the U–S–O–H–C system (Fig. 4), indicated once again that the biofilm is still depicted in the field of aqueous uranium(VI) sulfate complexation. Measurements of the water showed a redox potential of 480 ± 23 mV after 20 h and 373 ± 5 mV after 95 h. Although the pH of the water had been adjusted to a neutral pH twice the day the pH of the water decreased to 4.1 ± 0.1 and 4.3 ± 0.1 after 20 and 95 h, respectively. Experiments, which were performed without biofilms, did not show a decrease of the pH of the AMD water after its neutralization. Thus it can be assumed that the biofilm has an effect on the pH of the AMD water. Probably, the microbes of the biofilm are using different pH homeostatic mechanisms to maintain the intracellular pH. As described in Baker-Austin and Dopson (2007) the highly impermeable cell membrane of acidophiles is limiting the influx of protons into the cytoplasm. Additionally, intracellular mechanisms of the cytoplasm may buffer molecules sequester protons with the consequence that excess protons are removed from the cytoplasm by active proton pumping as described in Michels and Bakker (1985). Also, efflux systems (i.e. H^+ ATPase, antiporters and symporters) are possible. They are supporting the release of protons, identified in the sequenced genomes of the *Ferroplasma* type II and *Leptospirillum* group II, which

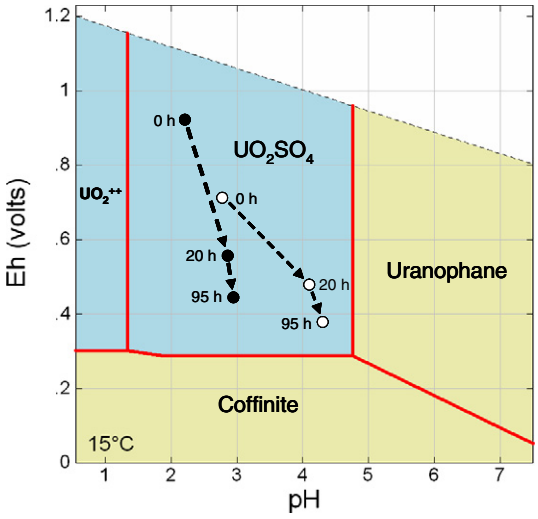

Fig. 4. Calculated ph–Eh diagram for U–S–O–H–C system at 15 °C. Eh and pH data of the macroscopic streamers (●) were plotted in comparison to the AMD solution (○) before, 20 and 95 h after the increase of the pH of the AMD water.

have been analyzed in an AMD biofilm from Iron Mountain, California (Tyson et al., 2004).

3.5. Staining experiments

Biofilm samples were stained with propidium iodide and DAPI before and immediately after the laboratory experiments, which were performed to simulate the first phase of the flooding process. The microscopic examinations of the samples by CLSM revealed that at the end of the experiment more than 50% of the bacteria fluoresce in the blue to cyan range at 461 nm, when excited with UV at 351 nm. This high proportion of DAPI stained bacteria indicates a natural stationary growth phase, which was determined 95 h after the neutralization experiments of the AMD water.

4. Conclusions

The results reveal that an immobilization of uranium in the biofilms as well as in the flooding water can be excluded for the most part in the uranium mine "Königstein" under the ambient conditions. Thermodynamic calculations and the plotting of the measured redox potential and pH into the pH–Eh diagram for the U–S–O–H–C system indicate that an aqueous uranium(VI) sulfate complex exists in the flooding water. Assuming, that the biofilm water will show a similar chemical composition, aqueous uranium(VI) sulfate complexation can be assumed in the biofilms, too. Since the uranium mine is currently in the process of being flooded the geochemical conditions will change by the inflow of water and the consequent increase of the pH of the flooding water. For an estimation of possible changes taking place during the first phase of the flooding process, laboratory experiments were performed, in which the pH of a flooding water sample was increased during 95 h in flow cells, filled with macroscopic streamers. A monitoring of the pH showed that the pH of the flooding water remained acid although it was permanently neutralized. We assume that the *F. myxofaciens* dominating biofilms have an effect on the acidification of the flooding water by using pH homeostatic mechanisms for example. As a consequence a bioremediation or immobilization of uranium in the biofilm as well as in the flooding water is prevented in the first phase of the flooding process. According to thermodynamic calculations a retention of uranium from the AMD water by forming solid uranium(VI) or uranium(IV) species will be inhibited until the pH will increase to >4.8. An upscaling of the laboratory results to the long-range situation in the galleries of the uranium mine during the flooding process is impossible due to the complexity of the geochemical parameters occurring in the uranium mine. However, it is expected that during a later phase of the flooding process the underground situation will change anyway, e.g. increase in pH, decrease of redox potential and reduced availability of oxygen. The modified geochemical condition may probably lead to a change of the microbial diversity. Consequently, the retention of uranium from the aqueous solution by the formation of a solid uranium species can be assumed.

Acknowledgments

The European Atomic Energy Community Seventh Framework Programme [FP7/2007–2013] under grant agreement n° 212287, Collaborative Project ReCosy and the German Research Council (DFG) (project no. AR 584/1-1) are thanked for funding. We thank R. Uebe and P. Luz from the Wismut GmbH for their cooperation and assistance in water and biofilm sampling. U. Schaefer and C. Eckardt are thanked for the analysis.

References

Abdelouas A, Lu Y, Lutze W, Nuttall HE. Reduction of U VI to U IV by indigenous bacteria in contaminated ground water. J Contam Hydrol 1998;35:217–33.
Arnold T, Baumann N, Krawczyk-Bärsch E, Brockmann S, Zimmermann U, Jenk U, et al. Identification of the uranium speciation in an underground acid mine drainage environment analysed by laser fluorescence spectroscopy. Geochemica et Cosmochimica Acta 2011;75:2200–12.
Baker-Austin C, Dopson M. Life in acid: pH homeostasis in acidophiles. Trends Microbiol 2007;15(4):165–71.
Beyenal H, Sani RK, Peyton BM, Dohnalkova AC, Amonette JE, Lewandowski Z. Uranium immobilization by sulfate-reducing biofilms. Environ Sci Technol 2004;38:2067–74.
Brockmann S, Arnold T, Schweder B, Bernhard G. Visualizing acidophilic microorganisms in biofilm communities using acid stable fluorescence dyes. J Fluoresc 2010;20(4):943–51.
Chen F, Ewing RC, Clark SE. The Gibbs free energies and enthalpies of formation of $U6^+$ phases: an empirical method of prediction. American Mineralogist 1999;84:650–64.
Clark SB, Ewing RC, Schaumloffel JC. A method to predict free energies of formation of mineral phases in the U(VI)–SiO_2–H_2O system. J. Alloys Comp. 1998;271:189–93.
de Beer D. Potentiometric microsensors for in situ measurements in aquatic environments. In: Buffle J, Horvai G, editors. In situ monitoring of aquatic systems. Chichester: Wiley; 2000. p. 161–94.
España JS, Pamo EL, Santofimia E, Aduvire O, Reyes J, Barettino D. Acid mine drainage in the Iberian Pyrite Belt (Odiel river watershed, Huelva, SW Spain): geochemistry, mineralogy and environmental implications. Applied Geochemistry 2005;20:1320–56.
Flemming H-C. Sorption sites in biofilms. Wat. Sci. Tech. 1995;32:27–33.
Gorman-Lewis D, Mazeina L, Fein JB, Szymanowski JES, Burns PC, Navrotsky A. Thermodynamic properties of soddyite from solubility and calorimetry measurements. J. Chem. Thermodynamics 2007;39:568–75.
Gorman-Lewis D, Fein JB, Burns PC, Szymanowski JES, Converse J. Solubility measurements of the uranyl hydrate phases metaschoepite, compreignacite, Na-compreignacite, becquerelite, and clarkeite. J. Chem. Thermodynamics 2008;40:980–90.
Grossmann K, Arnold A, Krawczyk-Bärsch E, Diessner S, Wobus A, Bernhard G, et al. Identification of fluorescent U(V) and U(VI) microparticles in a multispecies biofilm by confocal laser scanning microscopy and fluorescence spectroscopy. Environ Sci Technol 2007;41:6498–504.
Guillaumont R, Fanghänel T, Fuger J, Grenthe I, Neck V, Palmer DA, Rand MH. Update on the chemical thermodynamics of uranium, neptunium, plutonium, americium and technetium. In: OECD Nuclear Energy Agency, editor. In Chemical Thermodynamics. Amsterdam: Elsevier; 2003. Vol.5.
Hallberg KB, Johnson DB. Novel acidophiles isolated from moderately acidic mine drainage waters. Hydrometallurgy 2003;71:139–48.
Hallberg KB, Coupland K, Kimura S, Johnson DB. Macroscopic streamer growths in acidic, metal-rich mine waters in north Wales consist of novel and remarkably simple bacterial communities. Appl Environ Microbiol 2006;72(3):2022–30.
Kirby CS, Thomas HM, Southam G, Donald R. Relative contributions of abiotic and biological factors in Fe(II) oxidation in mine drainage. Appl. Geochem. 1999;14:511–30.
Kühl M. Optical microsensors for analysis of microbial communities. In: Leadbetter JR, editor. In environmental microbiology, vol. 397. Methods in Enzymology; 2005. p. 166–99.
Krawczyk-Bärsch E, Grossmann K, Arnold T, Hofmann S, Wobus A. Influence of uranium (VI) on the metabolic activity of stable multispecies biofilms studied by oxygen

microsensors and fluorescence microscopy. Geochimica et Cosmochimica Acta 2008;72:5251–65.
Lünsdorf H, Strömpel C, Osborn AM, Bennasar A, Moore ERB, Abraham W-R, et al. Hydrophobic substrates, and soil colloids leading to formation of composite biofilms, and to study initial events in microbiogeological processes. Methods in Enzymology 2001;331:317–31.
Macaskie LE, Bonthrone KM, Yong P, Goddard DT. Enzymically mediated bioprecipitation of uranium by a *Citrobacter* sp.: a concerted role for exocellular lipopolysaccharide and associated phosphatase in biomineral formation. Microbiology 2000;146:1855–67.
Merroun ML, Raff J, Rossberg A, Hennig C, Reich T, Selenska-Pobell S. Complexation of uranium by cells and S-layer sheets of *Bacillus sphaericus* JG-A12. App. Environ. Microbiol. 2005;71(9):5532–43.
Michels M, Bakker EP. Generation of a large, protonophore-sensitive proton motive force and pH difference in the acidophilic bacteria *Thermoplasma acidophilum* and *Bacillus acidocaldarius*. J Bacteriol 1985;161:231–7.
Nguyen AN, Silvac RJ, Weed HC, Andrews JW. Standard Gibbs free energies of formation at the temperature 303.15 K of four uranyl silicates: soddyite, uranophane, sodium boltwoodite, and sodium weeksite. Journal of chemical thermodynamics 1992;24 (4):359–76.
Pisarowicz JA, de Villa Luz Cueva. An active case of H_2S speleogenesis. In: Sasowsky ID, Palmer MV, editors. In breakthroughs in Karst geomicrobiology and redox geochemistry. Karst Waters Institute; 1994. p. 60–2.
Pons MP, Fusté MC. Uranium uptake by immobilized cells of *Pseudomonas* strain EPS 5028. Appl Microbiol Biotechnol 1993;39:661–5.
Rawlings DE, Tributsch H, Hansford GS. Reasons why "Leptospirillum"-like species rather than *Thiobacillus ferrooxidans* are the dominant iron-oxidizing bacteria in many commercial processes for the biooxidation of pyrite and related ores. Microbiology 1999;145:5-13.
Reimer L, Zepke U, Moesch J, Schulze-Hillert S, Ross-Messemer M, Probst W, et al. EELSpectroscopy. A reference handbook of standard data for identification and interpretation of electron energy loss spectra and for generation of electron spectroscopic images. Oberkochen, Germany: Institute of Physics, University of Münster, Germany, and Carl Zeiss, Electron Optics Division; 1992.
Revsbech NP. Analysis of microbial communities with electrochemical microsensors and microscale biosensors. Methods Enzymol 2005;397:147–66.
Seifert J, Erler B, Seibt K, Rohrbach N, Arnold J, Schlömann M, et al. Characterization of the microbial diversity in the abandoned uranium mine Königstein. In: Merkel B, Hasche-Berger A, editors. In uranium, mining and hydrogeology. Berlin, Heidelberg: Springer; 2008. p. 733–42.
Späth R, Flemming H-C, Wuertz S. Sorption properties of biofilms. Wat. Sci. Technol. 1998;37:207–10.
Spurr AR. A low viscosity epoxy resin embedding medium for electron microscopy. Ultrastruct. 1969;26:31–43.
Stoodley P, de Beer D, Lewandowski Z. Liquid flow in biofilm systems. Appl Environ Microbiol 1994;60(8):2711–6.
Stumm W, Morgan JJ. Aquatic chemistry, chemical equilibria and rates in natural waters. 3rd ed. New York: John Wiley & Sons, Inc.; 1996.
Tyson GW, Chapman J, Hugenholtz P, Allen EE, Ram RJ, Richardson PM, et al. Community structure and metabolism through reconstruction of microbial genomes from the environment. Nature 2004;428:37–43.
Vilalta E, Sabater S. Structural heterogeneity in cyanobacterial mats is associated with geosmin production in rivers. Phycologia 2005;44(6):678–84.
Wilson WD, Tanious FA, Barton HJ, Jones RL, Fox K, Wydra RL, et al. DNA sequence dependent binding modes of 4′,6-diamidin-2-phenylindole (DAPI). Biochemistry 1990;29:8452–61.
Ziegler S, Ackermann S, Majzlan J, Gescher J. Matrix composition and community structure analysis of a novel bacterial pyrite leaching community. Environ Microbiol 2009;11(9):2329–38.